Articles in PresS. J Neurophysiol (July 26, 2006). doi:10.1152/jn.00425.2006

FINAL ACCEPTED VERSION

Origins of cross-orientation suppression in the visual cortex

Baowang Li, Jeffrey K. Thompson, Thang Duong, Matthew R. Peterson, Ralph D. Freeman

Group in Vision Science, School of Optometry, Helen Wills Neuroscience Institute, University of California, Berkeley, CA 94720-2020

Corresponding author:
Ralph D. Freeman
360 Minor Hall
University of California, Berkeley
Berkeley, CA 94720-2020
E-mail: freeman@neurovision.berkeley.edu

Running head: Cross-orientation suppression in visual cortex

Abstract

The response of a neuron in striate cortex to an optimally oriented stimulus is suppressed by a superimposed orthogonal stimulus. The neural mechanism underlying this cross orientation suppression (COS) may arise from intracortical or subcortical processes or from both. Recent studies of the temporal frequency and adaptation properties of COS suggest that depression at thalamo-cortical synapses may be the principal mechanism. To examine the possible role of synaptic depression in relation to COS, we measured the recovery time course of COS. We find it too rapid to be explained by synaptic depression. We also investigated potential subcortical processes by measuring single cell contrast response functions for a population of LGN neurons. In general, contrast saturation is a consistent property of LGN neurons. Combined with rectifying nonlinearities in the LGN and spike threshold nonlinearities in visual cortex, contrast saturation in the LGN can account for most of theCOS that is observed in the visual cortex.

Keywords: contrast saturation, LGN, visual cortex, synaptic depression

Introduction

The response of a neuron in striate cortex to an optimally oriented *test* grating is attenuated by an overlapping orthogonal *mask* grating (Morrone et al. 1982; Morrone et al. 1987). The mask does not have to be perpendicular as it suppresses response to the test grating over a wide range of orientations (Bonds 1989; DeAngelis et al. 1992; Morrone et al. 1982). This *cross-orientation suppression* (COS) has been studied extensively, and it has generally been thought to be due to intracortical inhibition (Blakemore and Tobin 1972; Bonds 1989; Carandini and Heeger 1994; Carandini et al. 1997; DeAngelis et al. 1992; Heeger 1992; Morrone et al. 1982; Morrone et al. 1987; Sengpiel et al. 1998). The mechanism of COS has functional implications because it may play a role in important properties of visual cortical neurons, such as the refinement of orientation selectivity (Carandini and Ringach 1997; Chapman and Stryker 1992; Lauritzen et al. 2001; Somers et al. 1995; Vidyasagar et al. 1996), and spatial frequency selectivity (Bauman and Bonds 1991), and as a component of contrast normalization (Carandini and Heeger 1994; Heeger 1992).

Since COS can be induced by a wide range of mask orientations and spatial frequencies, and cells in the LGN are also broadly tuned for these parameters, it is plausible that the mechanism for COS originates in the LGN (Bonds 1989; DeAngelis et al. 1992; Walker et al. 1998). However, this explanation is not consistent with the experimentally demonstrated lack of COS in LGN cells (Bauman and Bonds 1991) and the fact that geniculate afferents to the visual cortex appear to be exclusively excitatory (Creutzfeldt and Ito 1968; Garey and Powell 1971; Tanaka 1985). Based on these arguments, several studies have concluded that the source of COS is intracortical

inhibition from a pool of cortical neurons exhibiting a wide range of orientation and spatial frequency preferences (Bauman and Bonds 1991; Bonds 1989; DeAngelis et al. 1992; Heeger 1992; Morrone et al. 1982; Sengpiel et al. 1998; Walker et al. 1998).

In recent work, synaptic depression at thalamo-cortical synapses has been proposed as the mechanism underlying COS in the visual cortex (Carandini et al. 2002; Freeman et al. 2002; Mrsic-Flogel and Hubener 2002). Synaptic depression is a form of short-term synaptic plasticity in which the efficacy of a given synapse is temporarily reduced according to its recent activity level (Abbott and Nelson 2000; Chance et al. 1998). However, there are temporal aspects of synaptic depression in relation to COS that require examination. In the study reported here, we have investigated the recovery time course of COS and find it inconsistent with typical temporal properties of synaptic depression. This makes it unlikely that synaptic depression is a major mechanism underlying COS in the visual cortex.

As an alternative to the synaptic depression hypothesis, we propose a feed-forward mechanism for COS, in which suppression originates in the LGN through a rectifying nonlinearity and contrast saturation, and that COS is strengthened in the visual cortex by a spike threshold nonlinearity. Our measurements of contrast saturation in LGN are consistent with this notion. Following the conclusion of our experimental work, two relevant publications have appeared. In one, intracellular techniques were used to investigate COS (Priebe and Ferster 2006). The main finding was that cross oriented stimuli suppressed both synaptic inhibition and synaptic excitation. A feed-forward model provided a prediction of COS. In the second study, COS was found to be rapid.

From other temporal measurements, COS was suggested to be caused by feed-forward signals or rapid intracortical neuronal paths (Smith et al. 2006).

Materials and Methods

Physiological preparation

All procedures complied with the National Institutes of Health Guide for the Care and Use of Laboratory Animals. Extracellular recordings are made with epoxy coated tungsten microelectrodes (A-M Systems, WA, USA) in the striate cortex of anesthetized and paralyzed mature cats (5-8 months, 2.5-3.5Kg). Anesthesia is induced with thiopental sodium intravenously and maintained at an appropriate rate determined individually for each cat. A tracheal cannula is positioned and the animal is artificially ventilated (25% O_2, 75% N_2O) at a rate adjusted to maintain expired CO_2 at 4-5%. Temperature is maintained at 38^{o}C. After the anesthetic level is stabilized at a constant rate of thiopental sodium, the cat is paralyzed with an intravenous infusion of pancuronium bromide (0.2 mg. kg^{-1}. hr^{-1}). EEG, ECG, heart rate, temperature, and end-tidal CO_2 are monitored during the experiment. A craniotomy is performed over area 17 and LGN. The dura is resected and covered with agar and wax to prevent drying and to reduce pulsation. For area 17 recording, electrode penetrations are made along the medial bank of the postlateral gyrus, 4mm posterior and 2mm lateral from the Horsley-Clarke origin (Horsley and Clarke 1908) at an angle of 10 degrees medial and 20 degrees anterior. For LGN recording, vertical electrode penetrations are made 6mm anterior and 9mm lateral from H-C zero. Small position adjustments of our electrodes are made in order to enter the LGN near the representation of the area centralis.

Extracellular recordings

Single units are isolated by the shapes of their spike waveforms. Initial estimates of each neuron's tuning parameters are obtained qualitatively using computer-controlled manipulation of drifting sinusoidal gratings. Quantitative measurements of tuning functions for orientation, spatial frequency, temporal frequency, size, ocular dominance, and stimulus contrast are then performed. Response amplitude is taken as the mean firing rate for complex cells or as the mean amplitude of the first harmonic of the response for simple cells and LGN cells. Since contrast gain and dynamic response range are apparently similar for X and Y cells (Hartveit and Heggelund 1992), we did not use this classification system for our LGN cell sample. The stimuli are presented to the dominant eye (responsive eye for LGN cells) while the nondominant eye (unresponsive eye for LGN cells) views a blank CRT screen of the same mean luminance as the gratings.

Recovery time course of COS

After the initial characterization of a cell in area 17, we examined the responses to an optimal test stimulus before, during and after the presentation of an orthogonal mask, as illustrated in Fig.1. Test and mask stimuli are sinusoidal drifting gratings at optimal and orthogonal orientations, respectively. The temporal frequencies of the mask stimuli are pre-determined through a separate protocol (Allison et al. 2001; Freeman et al. 2002; Li et al. 2005). In brief, the temporal frequency of the test grating is fixed to the optimal for the cell while that of the mask is varied from 0.5 to 25 Hz. The temporal frequency that elicits maximum suppression is used for the mask stimulus in this experiment. For our population of cells, 4-10 Hz produced maximum COS values. In order to examine the recovery time course of COS, we measured the response to the test stimulus following

presentation of a 0.5-second mask. After the mask is presented, five delay periods are used prior to the test stimulus (0, 0.5, 1, 2, 4 seconds as depicted in Fig.1C). We also measured responses to test-only (Fig. 1A) and to test plus mask (i.e., plaid) conditions (Fig.1B). Presentations are randomized with 10-second inter-stimulus intervals. Blank trials(i.e. no stimulus) are also interleaved with stimulus presentations. The contrast of both the test and mask is 50%. The entire condition set is repeated 10-20 times and responses are averaged across trials.

Results

We recorded from a total of 160 cells. Of these, 89 were from LGN and 71 were from visual cortex. Of the cortical cells, 25 and 46 were classified as simple and complex types, respectively.

Recovery time course of COS

In order to consider synaptic depression as a principal mechanism of COS, we first note a predicted recovery time course that this process would require. Specifically, responses to the test stimulus following a mask should recover exponentially toward the test-only response condition (Abbott et al. 1997; Chance et al. 1998; Varela et al. 1997). This prediction is quantified as:

$$R(t) = a-(a-b)\times e^{-t/T} \quad (1)$$

where *R* represents the response of the neuron to the test stimulus following the mask, *a* is the mean response to the test-only stimulus, *b* is the mean response to the plaid stimulus, and *T* is the time constant for synaptic depression (Abbott et al. 1997; Chance et al. 1998; Varela et al. 1997).

Reported time constants for a fast form of synaptic depression are generally between 200 and 600 ms (Abbott et al. 1997; Chance et al. 1998; Varela et al. 1997). In our analysis, we use these values (i.e., T=200ms and 600ms) as upper and lower bounds to predict the responses of cortical cells. To make these predictions suitable for our measurements, we average R(t) across the first 500ms of each response.

Figure 2A shows data from a representative cortical simple cell where the responses are plotted as a function of the delay between mask and test stimuli. The top and bottom horizontal dashed lines represent responses to the test and plaid, respectively. Dotted lines above and below the dashed lines represent ±1SE of the mean value. All responses represent the average neural spike rate during the first 500ms of the test stimulus. This example cell exhibits clear suppression to the plaid stimulus. The mean responses to the test (top dashed line) and plaid (bottom dashed line) are 42.8 and 23.9 spikes/s respectively, i.e., there is a 44% response reduction when the mask is superimposed on the test stimulus. If the mechanism underlying this suppression were synaptic depression, we would expect the response to the test stimulus to be reduced for some period following removal of the mask since synaptic depression is known to have a prolonged recovery time (Abbott et al. 1997; Chance et al. 1998; Varela et al. 1997; Varela et al. 1999). However, responses to the test grating for all temporal delay conditions (0, 0.5, 1, 2, or 4s, unfilled circles) are nearly identical to those of the test-only condition (top dashed line).

This result is consistent across a population of cortical cells (n=36). The mean response curve for all cells tested is shown in Figure 2B in which responses are normalized by the response to the test-only condition. On average, a simultaneously

presented mask stimulus suppresses the response to a test stimulus by 42% (mean normalized response = 0.58±0.05, SEM). However, the mean normalized response to the test following mask stimulus is 1.05±0.05. This demonstrates that recovery from the suppressive effects of the mask is very rapid. To quantify this effect across our population we calculate the magnitude of recovery for each response and express it as a percentage of the suppression induced by the plaid. Figure 2C is a population histogram of the values we obtained for the 0s delay condition. A value of 100% represents complete recovery, whereas 0% indicates the response is suppressed to the same degree as that of the plaid. Consistent with the data of Figure 2B, the responses of most neurons (20 of 36) are essentially unaffected by the preceding mask stimulus (percent recovery ≈ 100%). This applies equally to both simple and complex cells (p=0.5, t-test). A model of synaptic depression predicts percent recovery values between 60% and 30% (up and down triangles) for assumed time constants of 200 and 600 ms (Abbott et al. 1997; Chance et al. 1998; Varela et al. 1997), respectively. These results suggest that synaptic depression processes are too slow to account for the rapid recovery from a briefly presented mask stimulus.

The data presented in Figure 2A-C depict response magnitudes averaged over a 0.5s time window. However, this analysis may be insensitive to rapid changes mediated by especially fast forms of short-term synaptic depression. To examine this possibility, we compare post-stimulus-time-histograms (PSTHs) for the following three stimulus conditions: 1) the test-only stimulus (Figure 2D-E, unfilled circles), 2) the test stimulus following the mask (0s delay condition) (Figure 2D-E, filled circles), and 3) the plaid stimulus (Figure 2D-E, unfilled squares). Only responses from complex cells are included

in this analysis since the onsets of simple cell responses are related to the phase of the drifting grating and are therefore not suitable for resolving fast response onset times. Results for a representative complex cell are given in Figure 2D and the population averaged responses are shown in Figure 2E. Consistent with the above analysis, there is no significant difference between the test-only response time course (unfilled circles) and the test following mask response time course (filled circles). This is the case even during the first 100ms of the response. For comparison, the response to the plaid stimulus is clearly suppressed at these early time points. If COS in visual cortex were mediated by synaptic depression, we would expect a mask stimulus to induce suppression during the initial part of a subsequent test stimulus. However, there is no evidence of this type of suppression.

Finally, we note that studies of cells in visual cortex in which stimuli have been presented in random sequence show that firing rate increases have relatively long latencies (~20ms) compared to decreases (Bair et al. 2002; Smith et al. 2001). This delay has been cited as evidence in support of a model of synaptic depression (Carandini et al. 2002; Freeman et al. 2002). However, 20ms is substantially shorter than the recovery times for synaptic depression typically reported in the literature (Abbott et al. 1997; Chance et al. 1998; Varela et al. 1997; Varela et al. 1999). Furthermore, the origin of this delay is not clear since a number of different mechanisms could cause a delay between the onset and offset of firing rates (Bair et al. 2002).

Linearity and the LGN

The analysis presented above shows thatsynaptic depression at thalamo -cortical synapses is unlikely to be the principal mechanism for COS in visual cortex. Other work on the temporal and adaptation properties of COS suggests that the primary mechanism underlying COS operates prior to the formation of cortical RFs (Freeman et al. 2002; Li et al. 2005; Sengpiel and Vorobyov 2005). Therefore, COS in visual cortex is likely to originate from the LGN itself, rather than thalamo-cortical synapses. Previous studies of COS have generally overlooked the response nonlinearity of neurons in the LGN (Bonds 1989; Carandini and Heeger 1994; DeAngelis et al. 1992; Sengpiel et al. 1998; Walker et al. 1998).There are two major nonlinear inputs from LGN cells to cortical simple cells: spike rectification and contrast saturation in the LGN. The former refers to the fact that LGN responses cannot be decreased below zero and the latter obtains because LGN cells do not generally respond proportionally to stimulus contrast. Although contrast saturation in LGN neurons is less pronounced than that in visual cortex (Ohzawa et al. 1985; Sclar et al. 1990), an assumption of linearity is not warranted. To determine the degree of nonlinearity, we measured contrast response functions for a population of cells in the LGN (n=74) for a wide range of contrast levels (1, 2, 4, 7, 14, 26, 50, and 100%).

Figure 3A shows an example LGN contrast response function that exhibits a modest degree of saturation (unfilled circles). The firing rates at 50% and 100% contrast are 86 and 91 spikes/s respectively. A neuron without contrast saturation would exhibit a substantially larger response at 100% contrast (172 spikes/s) based on its response to the 50% contrast stimulus. To quantify the effects of contrast saturation, we calculated a contrast saturation index (CSI). This index is based on neural responses to two successive and adjacent contrast values that are used to determine contrast response functions. The

lower of two successive levels is used to predict responses to the higher contrasts. This prediction, based on the assumption of a linear contrast response function, is then compared to the measured response. CSI values of 0 and 0.5 represent, respectively, linear and full contrast saturation. Formally, CSI is defined as:

$$CSI = 1.0 - R_{measured} / R_{predicted} \quad (2)$$

Where $R_{measured}$ and $R_{predicted}$ are, respectively, measured and predicted responses, as described above.

The example cell in Figure 3A exhibits contrast saturation over a wide range of contrast levels. For contrasts above 7%, CSI increases monotonically with stimulus contrast (filled circles, dashed lines). Different levels of contrast saturation are observed across our population of LGN cells. Figure 3B shows the distribution of CSI values for the 50% and 100% response pairs. In our sample, the mean CSI is 0.33 ± 0.02 (SEM, n=74). This indicates that contrast saturation isa consistent property of LGN cells . To investigate the contrast saturation properties for different contrast levels, CSIs are calculated for two adjacent contrasts (Figure 3C). The numbers of cells for 7 and 14%, 14 and 26%, 26 and 50%, and 50 and 100% contrasts are 44, 70, 74 and 74, respectively. In all cases, contrast pairs are used only for responses which are significant ($p \leq 0.05$, t-test). Consistent with the example cell for which data are shown in Figure 3A, the strength of contrast saturation increases approximately monotonically with stimulus contrast.

Predicted suppression through a feed-forward model

The experimental data we present here show clearly that COS in visual cortex recovers rapidly after the presentation of a mask stimulus (Figure 2) and that most

neurons in the LGN exhibit some degree of contrast saturation (Figure 3). The first result suggests that synaptic depression is unlikely to be the principal source of COS in the visual cortex. The second finding indicates that contrast saturation at the LGN level may play an important role in COS. To explore this possibility, we use a physiologically plausible model to propose that COS arises from response nonlinearities of LGN cells and is strengthened in visual cortex by spike threshold nonlinearities.

Our model follows the serial processing notion by which orientation selectivity is derived from excitatory LGN input (Hubel and Wiesel 1962; Reid and Alonso 1995). It follows closely the costruction of a previous model used to explore synaptic depression in visual cortex (Carandini et al. 2002). The cortical simple cell receptive field is determined by thalamocortical excitaiton. ON and OFF cortical RF subregions arise from ON-center and OFF-center LGN cells. The excitation is accompanied by subtractive inhibition of a "push-pull" form. Both excitation and inhibition are included via ON-center and OFF-center neurons. Although intracortical inhibition could be included in this construction (Palmer and Davis 1981; Troyer et al. 1998) our approach is for inhibition to be derived exclusively from LGN. In our model, LGN cells operate linearly but have an added nonlinearity. The nonlinearity is established by assuming a resting spike rate of LGN cells of 10 spikes/sec (Carandini et al. 2002) and a contrast saturation component as conveyed in Figure 3. For each LGN cell in our model, the contrast saturation nonlinearity is estimated by using the mean normalized contrast response function from all LGN cells (n=74). This contrast response function is well fit (the goodness of fit $R_{square} = 0.99$) with a hyperbolic ratio function, $R = 1.0 \times C/(C+C_{50})$, where C and C_{50} represent stimulus contrast and the contrast level that elicts half of maximum response,

respectively. The estimated value of C_{50} from our population of LGN cells is 27.8%. Consistent with the model in the previous study (Carandini et al., 2002), we assume that the maximum modulation response of LGN cells is 100 spikes/sec. However, in our model, thalamo-cortical synapses operate in a linear manner, i.e.,synaptic depression is not included. We also assume that there is a spiking mechanism for cortical cells and that the firing rate is a rectified version of the membrane potential with a threshold of 5 spikes/sec (Anderson et al. 2000; Carandini and Ferster 2000; Carandini et al. 2002).

In our model, depicted in Fig. 4A, summation of LGN inputs occurs in a "push-pull" manner. In this configuration, excitation from an ON-center LGN cell and inhibition from an OFF-center LGN cell form an ON subregion. Likewise, excitation from an OFF-center and inhibition from an ON-center LGN cell form an OFF subregion (Carandini and Heeger 1994; Carandini et al. 1997; Glezer et al. 1982; Tolhurst and Dean 1990). Although inhibition is thought to operate through cortical inhibitory interneurons (Palmer and Davis 1981; Troyer et al. 1998), for our present purpose, it is assumed to come directly from LGN cells. This assumption is for simplicity. Intracortical inhibitory connections included in other models (Albrecht and Geisler 1991; Ben-Yishai et al. 1995; Carandini and Heeger 1994; Carandini and Ringach 1997; Heeger 1992; McLaughlin et al. 2003; McLaughlin et al. 2000; Shelley and McLaughlin 2002; Shelley et al. 2002; Wielaard et al. 2001) are not considered in our current analysis since they do not appear to be relevant to COS (Freeman et al. 2002; Li et al. 2005; Sengpiel and Vorobyov 2005). We assume that test and mask stimuli are sinusoidal drifting gratings which are vertical and horizontal, respectively. The contrast, duration, and temporal frequency of both test and mask stimuli are 50%, 2 second, and 4Hz, respectively. A plaid is formed by the

superposition of these gratings. The model simple cell responds to the test stimulus but not the mask. If LGN cells respond linearly to a visual stimulus, a simutaneuous presentation of the mask will not affect the synaptic input to the model simple cell. However, with spike rectification and contrast saturation in the LGN, synaptic input to the model simple cell is assumed to be reduced by the mask.

The first stage of our model consists of a standard feed-forward process for the generation of simple cell RFs in visual cortex (Fig. 4A). The RF of the simple cell is modeled to receive inputs from 50 LGN cells. LGN cells are spatially distributed 5×5 across the simple cell receptive field, for which the orientation selectivityto vertical orientations arises from the arrangement of excitatory LGN inputs. Summation of LGN inputs occurs in a push-pull manner, i.e., an excitation is supplemented by a subtractive inhibition through cortical inhibitory interneurons. For simplicity, we assume that inhibition is derived directly from the 5×5 array of LGN cells that feed the model simple cell. Eight LGN neurons are represented in Fig. 4A, B. Four of the eight LGN cells provide "push" excitatory input to the cortical cell. The remaining four LGN cells provide "pull" inhibitory input to the cortical cell via inhibitory interneurons. Excitatory (or inhibitory) input consists of two ON-center and two OFF-center LGN cells with ON-center cells in the ON (or OFF) and OFF-center cells in the OFF (or ON) subfield of the cortical RF. Excitation by an ON-center cell is balanced by overlapping inhibition from an OFF-center cell. Figure 4B illustrates how contrast saturation in the LGN may lead to COS in visual cortex. The model simple cell gives a maximum response (4) to a vertical grating and no response (0) to a horizontal grating. We consider two possible outcomes when both gratings are presented simultaneously in orthogonal orientations. First, if LGN

cells respond linearly to stimulus contrast, the response of the cortical cell will be the same as that to a vertical grating alone (i.e., (4)). However, if cells in the LGN exhibit contrast saturation as shown in Fig. 3, the response of the cortical cell will be reduced (<4).

As shown above, contrast saturation is present in LGN neurons (Figure 3). We apply the contrast response nonlinearity (spike rectification and contrast saturation) for each LGN cell in our model to predict the level of COS in visual cortex. Normalized responses of the model cortical cell are shown in Figure 4C. The two bars labeled *test* and *mask* represent, respectively, the normalized responses of the model cortical neuron to test and mask presentations at 50% contrast levels. The bar labeled *predicted* represents the predicted responses to the plaid based on a population of LGN neurons exhibiting the mean contrast saturation observed in this study (CSI = 0.33). In this case, the predicted response is 0.60, i.e.,the plaidsuppress es the response of the cell by40%. This represents a strength of suppression that is 7% higher than the mean contrast saturation (0.33) we observe in LGN. This difference may be accounted for by a rectifying nonlinearity of LGN cells and a spike output nonlinearity of cortical cells. The fourth bar in Fig 4C, labeled *measured,* represents the mean response to the plaid, which is normalized by the response to the test-only condition averaged across the entire 2s stimulus duration (n=36, see Figure 2B). In this case, we observe a response reduction of 49% relative to the test-only condition. This is close to the predicted strength of COS (40 %) from the model cortical cell and consistent with our previous report of COS (Walker et al., 1998). Therefore, if we incorporate a rectifying nonlinearity for LGN cells and a spike threshold

nonlinearity for cortical cells, then contrast saturation in the LGN can account for most COS in cortical cells for high contrast conditions.

Since the CSI in LGN increases with stimulus contrast (Fig. 3C), our model predicts that the level of suppression increases with contrast. To test this prediction, we measured COS for 35 cortical cells at different test and mask contrasts. Figure 5A shows the normalized responses to different combinations of test and mask contrasts. The degree of suppression clearly increases with mask contrast and at very low values (less than 10%), the level of suppression is minimal. This is qualitatively consistent with our model prediction. To quantify this result, we compare the measured and predicted COS for mask and test stimuli that have equal contrast levels of 12.5, 25, and 50% (Figure 5B) . The gray bars depict the measured levels of suppression, whereas the black and white bars denote the mean CSI of LGN cells and predicted COS values, respectively. . Compared to measured COS levels, our model predicts 98.5%, 90.3% and 78.9% suppression for 12.5%, 25% and 50% contrasts, respectively. The data of Fig. 5 show that contrast saturation at the LGN level plays a reduced role at low contrast levels For 12.5%, 25% and 50% contrast levels, contrast saturation in the LGN can account for 24%, 47% and 84%, respectively, of the predicted COS. This result suggests that contrast saturation in the LGN may be the principal source of COS for high contrast levels, but for low contrasts other nonlinear mechanisms are important.

Contrast saturation in theLGN and temporal frequency

COS can be obtained with high temporal frequency mask stimuli that do not typically activate cortical cells (Allison et al. 2001; Freeman et al. 2002; Li et al. 2005;

Sengpiel and Vorobyov 2005). To explore this in our current study, and determine if this finding is consistent with our model, we measured contrast response functions at different temporal frequencies for a population of 15 LGN cells. Figure 6A showsresults for an example LGN cell. As the data show, there is contrast saturation for the tests at 7 and 10 Hz. Saturation also occurs at temporal frequencies of 2,4,15, and 25 Hz, but this is not obvious in Fig.6A since we use a standard logarithmic scale for contrast. We use the data at 50% and 100% contrasts to calculate CSI as a function of temporal frequency. This function is shown in Figure 6B for the example LGN cell. We quantify the tuning properties of this predicted suppression by fitting a Gaussian function to the temporal frequency tuning curve of CSI. We use this curve to calculate peak (TF_{peak}) and cutoff (TF_{cutoff}) temporal frequencies. TF_{cutoff} is defined as the temporal frequency at which the CSI value is reduced by half of that at TF_{peak}. The example cell exhibits a TF_{peak} of 8.6 Hz and a TF_{cutoff} value of 14.5 Hz. The distributions of TF_{peak} and TF_{cutoff} values for 15 LGN cells are presented in Fig. 6C, D. Although these temporal frequency tuning properties are broadly distributed, they are consistent with those of COS in visual cortex (Allison et al. 2001; Freeman et al. 2002; Li et al. 2005; Sengpiel and Vorobyov 2005). Considered together, these results are in accord with the hypothesis that contrast saturation in the LGN at high contrast levels may be the principal mechanism mediating COS in visual cortex.

Discussion

We have examined potential mechanisms of cross-orientation suppression (COS) in the visual cortex. A primary process proposed in previous work is synaptic depression. Recovery from synaptic depression typically requires several hundred milliseconds

(Abbott et al. 1997; Chance et al. 1998; Varela et al. 1997; Varela et al. 1999). Our current data show that the response to an optimal test stimulus is unaffected by a briefly presented orthogonal mask as long as the two stimuli do not overlap in time. This result, therefore, is inconsistent with a model in which synaptic depression is the principal source of COS. We find that contrast saturation in LGN cells, which has not been considered in previous studies (Carandini et al. 2002; Freeman et al. 2002), leads to strong COS in visual cortex for high contrast stimuli. This effect, in combination with the known rectifying nonlinearities in LGN and spike output nonlinearities of cortical neurons (Carandini 2004; Carandini and Ferster 2000; Priebe et al. 2004), can account for observed levels of COS in visual cortex. We have studied the saturation mechanism in LGN. However, this effect is likely to have a retinal origin. Retinal contrast gain control mechanisms are well established and they include the types of saturation effects we observe in LGN (Shapley and Victor 1978, 1979).

Recent work has shown that the temporal frequency and adaptation properties of cortical cells are not well matched to the characteristics of COS. COS can be induced by mask stimuli with higher temporal frequencies than those that can activate most cortical cells, and it is not affected by prolonged adaptation to mask stimuli (Freeman et al. 2002; Li et al. 2005; Sengpiel and Vorobyov 2005). These temporal frequency and adaptation properties are consistent with those of LGN neurons, but not cortical cells. Based on these results and the finding that COS is weak in the LGN (Bauman and Bonds 1991; Freeman et al. 2002), synaptic depression at thalamo-cortical synapses has been proposed as the mechanism underlying COS in the visual cortex (Carandini et al. 2002; Freeman et al. 2002; Mrsic-Flogel and Hubener 2002). Synaptic depression is a form of short-term

synaptic plasticity in which the efficacy of a given synapse is temporarily reduced according to its recent activity level (Abbott and Nelson 2000; Chance et al. 1998). *In vitro* studies have revealed at least two separate components of short-term synaptic depression acting over different time scales. A fast form occurs within 5-10 presynaptic action potentials and requires 200-600 ms for recovery, whereas a second slower form requires many action potentials to reach full strength and approximately 10s to fully recover (Chance et al. 1998; Varela et al. 1997; Varela et al. 1999). If synaptic depression underlies COS in the visual cortex, its temporal properties should be evident in the responses of cortical neurons. For example, if the slow form of synaptic depression were mediating COS we would expect to observe stronger suppression following prolonged adaptation to a mask stimulus. This is because synapses would become depressed during the adaptation period and remain depressed throughout the test period. In contrast, the response without prior adaptation would be high initially and exhibit suppression only at later time points, after synaptic depression had set in. Previous studies of COS do not support this prediction. COS is just as strong with prior adaptation as it is without (Freeman et al. 2002; Li et al. 2005; Sengpiel and Vorobyov 2005). This suggests that the slow form of synaptic depression with its prolonged onset time is not a viable mechanism for explaining COS.

Another prediction of the synaptic depression hypothesis is that test and mask stimuli need not to be presented simultaneously in order to observe COS. Since both fast and slow forms of synaptic depression exhibit significant recovery time constants, the suppressive effects of a mask stimulus should remain strong for at least a few hundred milliseconds following its removal. In the current study we evaluated this prediction for

neurons in the striate cortex. In contrast to the prediction, we find that both test and mask stimuli must be presented simultaneously in order to observe COS. This result suggests that neither form of synaptic depression is likely to be a dominant mechanism underlying COS in visual cortex.

In previous investigations, COS has been attributed to intracortical inhibition (Allison et al. 2001; Bauman and Bonds 1991; Bonds 1989; DeAngelis et al. 1992; Sengpiel et al. 1998). The primary evidence in support of this view is the finding that COS is blocked by application of the GABA agonist bicuculline over a large region of visual cortex (Morrone et al. 1987). However, this view has been questioned recently by data on the temporal frequency and adaptation properties of COS (Freeman et al. 2002; Li et al. 2005; Sengpiel and Vorobyov 2005). COS in the visual cortex can be obtained with a mask drifting too fast to elicit responses from most cortical cells (Freeman et al. 2002; Li et al. 2005; Sengpiel and Vorobyov 2005). In addition, COS is unaffected by adaptation to a mask grating, even though the responses of most cortical neurons are substantially suppressed by adaptation. These findings suggest that the primary mechanism underlying COS operates prior to the formation of cortical RFs (Freeman et al. 2002; Li et al. 2005; Sengpiel and Vorobyov 2005).

There are at least three plausible ways by which this could occur. The first possibility is that COSis present in LGN neurons and simply propagates to visual cortex. Although some cells in the LGN exhibit weak COS, it does not appear strong enough to explain the strength of suppression normally observed in visual cortex (Freeman et al. 2002). Furthermore, since LGN neurons are not selective for stimulus orientation, their responses to overlapping orthogonal stimuli are typically greater than those to either

stimulus in isolation (Freeman et al. 2002). A second possibility is that COS may be mediated at thalamo-cortical synapses through synaptic depression (Carandini et al. 2002; Freeman et al. 2002). This is somewhat complicated to verify since synaptic depression appears to be stronger *in vitro* than *in vivo* (Boudreau and Ferster 2005; Chung et al. 2002; Sanchez-Vives et al. 2000). However, based on the data and analysis reported here, this possibility also seems unlikely. A third possibility is that COS in visual cortex may originate from other subcortical nonlinear properties, such as rectifying nonlinearities and contrast saturation in LGN neurons as we propose here and as considered briefly in a previous study (Freeman et al. 2002).

The feed-forward model of COS postulated here is capable of explaining several of the properties of COS reported in previous studies (Bonds 1989; DeAngelis et al. 1992; Freeman et al. 2002; Li et al. 2005; Morrone et al. 1982). First, it accounts for the broad tuning of COS to mask orientation since LGN neurons do not exhibit orientation tuning. Second, it explains the fact that excitatory and suppressiveRFs are largely co-localized (DeAngelis et al. 1992). It is clear thatcontrast saturation occur s only when the mask stimulus is presented simultaneously on an overlapped region of the excitatory test stimulus. Contrast saturation would not occur if the mask and test stimuli were presented to different regions of the RF. Third, it accounts for the immunity of COS to prolonged mask adaptation (Freeman et al. 2002; Li et al. 2005; Sengpiel and Vorobyov 2005). LGN cells in the cat exhibit a small adaptation effect compared with cortical cells (Ohzawa et al. 1982, 1985; Sanchez-Vives et al. 2000; Shou et al. 1996). A prolonged mask grating will slightly shift the contrast response function of LGN cells to the right. This will reduce COS in visual cortex with a decrease of contrast saturation in the LGN

(see Figure 4B). On the other hand, the prolonged mask grating can decrease the firing rate of cortical cells (Carandini et al. 1998). These adaptation effects, which may reduce or increase COS, may offset each other. Finally, our model accounts for the temporal frequency properties of COS. It has been shown that COS can be obtained with mask stimuli drifting too rapidly to elicit substantial responses from cortical neurons (Allison et al. 2001; Freeman et al. 2002; Li et al. 2005; Sengpiel and Vorobyov 2005). Most LGN neurons exhibit strong contrast saturation to gratings at high temporal frequencies (Figure 6). This result is in agreement with the temporal frequency properties of COS in visual cortex (Allison et al. 2001; Freeman et al. 2002; Li et al. 2005; Sengpiel and Vorobyov 2005).

Results in the present study and previous investigations of temporal frequency and adaptation properties of LGN and cortical cells, point to subcortical mechanisms as the primary basis of COS (Freeman et al. 2002; Li et al. 2005; Sengpiel and Vorobyov 2005). With spike output nonlinearities attributable to cortical cells, our current findings suggest that rectifying nonlinearities and contrast saturation in the LGN can account for most COS in visual cortex. Of course, we cannot rule out the possible participation of other mechanisms such as synaptic depression, intracortical inhibition.

A recent paper casts doubt on a purely excitatory feed-forward mechanism for COS (Smith et al. 2006). Measurements were made of suppression, recovery, onset, and offset time courses for cortical neurons. COS and its release occurs quickly. However, it is delayed following the offset time response. This suggests a role for intracortical inhibition. However, to demonstrate this, inhibitory interneurons must be identified with the same temporal and adaptation properties as those for COS in visual cortex.

Another relevant issue concerns response phase advances with stimulus contrast increases. These have been reported in retina (Shapley and Victor 1978), LGN (Saul and Humphrey 1990), and visual cortex (Dean and Tolhurst 1986). When a mask is simultaneously presented with a test stimulus, the combination produces increased contrast. As a result, we should observe a phase advance of the response to the plaid in our experiments. However, phase advances are not evident in our data (Figs. 2D and E). Two possible reasons may account for this. First, the resolution (Figs. 2D and E) is not high enough to demonstrate phase advances in the response to the plaid. More spikes would be required from a number of repetitions to obtain higher resolution. Second, although synaptic depression is relevantly weak in vivo (Boudreau and Ferster 2005; Sanchez-Vives et al. 1998), phase delay from synaptic depression at thalamo-cortical synapses may cancel out the phase advance from the increased contrast in the plaid.

Species differences may also be relevant. In the primate, magnocellular but not parvocellular cells are reported to show contrast saturation (Benardete et al. 1992; Shapley et al. 1981). In addition, parvocellular cells appear to constitute the major input to visual cortex (Malpeli et al. 1996). COS has been demonstrated in primate visual cortex (Carandini et al. 1997). Therefore, it may be that contrast saturation from LGN cells is less of a factor in COS in the primate visual pathway.

A recently published study, in which intracellular techniques were used, reaches similar conclusions to ours regarding the origins of COS in the visual cortex (Priebe and Ferster 2006). In this study, excitatory and inhibitory conductances are both reduced about equally bythe overlapped mask. This suggests that cortico-cortical inhibition is not involved in COS. To explain COS, a toy model is also used in which there is feed-

forward excitation from thalamic relay cells to cortical simple cells. Within this model, contrast saturation and rectification of LGN cells are used to account for COS in simple cells for low and medium contrast levels (8 and 32%). However, this model produces elevated DC responses to the plaid stimulus (Table 1, Priebe and Ferster, 2006). Most likely, this is due to the use of a "push" only model. In our present study, we have used a "push-pull" architecture in which feed-forward excitation is balanced with anti-phase inhibition separated in spatial phase by 180 degrees. The inhibition is thought to be mediated by cortical interneurons (Carandini et al. 2002; Ferster 1988; Glezer et al. 1982; Palmer and Davis 1981; Tolhurst and Dean 1987; Troyer et al. 1998). Our model incorporates LGN rectification, contrast saturation and cortical spike threshold in a "push-pull" format where anti-phase inhibition balances feed-forward excitation. For low contrasts, this arrangement is appropriate. However, it is relatively less effective at high contrasts where other factors including cortico-cortical effects may operate. Overall, however, a "push-pull" approach seems preferable especially since it appears to be required to account for fundamental response characteristics of cortical neurons such as orientation tuning invariance (Sclar and Freeman 1982; Troyer et al. 1998).

In summary, we show here that synaptic depression at thalamo-cortical synapses is unlikely to be the primary mechanism in COS because it requires considerable recovery time. The combination of spike rectification and contrast saturation in the LGN and a spike output nonlinearity of cortical neurons into a standard "push-pull" feed-forward model can explain COS in visual cortex.

Acknowledgements

This work was supported by research and CORE grants (EY01175 and EY03716) from the National Eye Institute.

References

Abbott LF and Nelson SB. Synaptic plasticity: taming the beast. *Nat Neurosci* 3 Suppl: 1178-1183., 2000.

Abbott LF, Varela JA, Sen K, and Nelson SB. Synaptic depression and cortical gain control. *Science* 275: 220-224, 1997.

Albrecht DG and Geisler WS. Motion selectivity and the contrast-response function of simple cells in the visual cortex. *Vis Neurosci* 7: 531-546., 1991.

Albrecht DG and Hamilton DB. Striate cortex of monkey and cat: contrast response function. *J Neurophysiol* 48: 217-237., 1982.

Allison JD, Smith KR, and Bonds AB. Temporal-frequency tuning of cross-orientation suppression in the cat striate cortex. *Vis Neurosci* 18: 941-948, 2001.

Anderson JS, Lampl I, Gillespie DC, and Ferster D. The contribution of noise to contrast invariance of orientation tuning in cat visual cortex. *Science* 290: 1968-1972., 2000.

Bair W, Cavanaugh JR, Smith MA, and Movshon JA. The timing of response onset and offset in macaque visual neurons. *J Neurosci* 22: 3189-3205., 2002.

Bauman LA and Bonds AB. Inhibitory refinement of spatial frequency selectivity in single cells of the cat striate cortex. *Vision Res* 31: 933 -944, 1991.

Benardete EA, Kaplan E, and Knight BW. Contrast gain control in the primate retina: P cells are not X-like, some M cells are. *Vis Neurosci* 8: 483-486., 1992.

Ben-Yishai R, Bar-Or RL, and Sompolinsky H. Theory of orientation tuning in visual cortex. *Proc Natl Acad Sci U S A* 92: 3844-3848., 1995.

Blakemore C and Tobin EA. Lateral inhibition between orientation detectors in the cat's visual cortex. *Exp Brain Res* 15: 439-440, 1972.

Bonds AB. Role of inhibition in the specification of orientation selectivity of cells in the cat striate cortex. *Vis Neurosci* 2: 41-55, 1989.

Boudreau CE and Ferster D. Short-term depression in thalamocortical synapses of cat primary visual cortex. *J Neurosci* 25: 7179-7190., 2005.

Carandini M. Amplification of trial-to-trial response variability by neurons in visual cortex. *PLoS Biol* 2: E264. Epub 2004 Aug 2024., 2004.

Carandini M and Ferster D. Membrane potential and firing rate in cat primary visual cortex. *J Neurosci* 20: 470-484., 2000.

Carandini M and Heeger DJ. Summation and division by neurons in primate visual cortex. *Science* 264: 1333-1336, 1994.

Carandini M, Heeger DJ, and Movshon JA. Linearity and normalization in simple cells of the macaque primary visual cortex. *J Neurosci* 17: 8621-8644., 1997.

Carandini M, Heeger DJ, and Senn W. A synaptic explanation of suppression in visual cortex. *J Neurosci* 22: 10053-10065, 2002.

Carandini M, Movshon JA, and Ferster D. Pattern adaptation and cross-orientation interactions in the primary visual cortex. *Neuropharmacology* 37: 501-511, 1998.

Carandini M and Ringach DL. Predictions of a recurrent model of orientation selectivity. *Vision Res*37: 3061 -3071., 1997.

Chance FS, Nelson SB, and Abbott LF. Synaptic depression and the temporal response characteristics of V1 cells. *J Neurosci* 18: 4785-4799, 1998.

Chapman B and Stryker MP. Origin of orientation tuning in the visual cortex. *Curr Opin Neurobiol* 2: 498-501., 1992.

Chung S, Li X, and Nelson SB. Short-term depression at thalamocortical synapses contributes to rapid adaptation of cortical sensory responses in vivo. *Neuron* 34: 437-446, 2002.

Creutzfeldt O and Ito M. Functional synaptic organization of primary visual cortex neurones in the cat. *Exp Brain Res* 6: 324-352, 1968.

Dean AF and Tolhurst DJ. Factors influencing the temporal phase of response to bar and grating stimuli for simple cells in the cat striate cortex. *Exp Brain Res* 62: 143-151, 1986.

DeAngelis GC, Robson JG, Ohzawa I, and Freeman RD. Organization of suppression in receptive fields of neurons in cat visual cortex. *J Neurophysiol* 68: 144-163, 1992.

Ferster D. Spatially opponent excitation and inhibition in simple cells of the cat visual cortex. *J Neurosci* 8: 1172-1180., 1988.

Freeman TC, Durand S, Kiper DC, and Carandini M. Suppression without inhibition in visual cortex. *Neuron* 35: 759-771, 2002.

Garey LJ and Powell TP. An experimental study of the termination of the lateral geniculo-cortical pathway in the cat and monkey. *Proc R Soc Lond B Biol Sci* 179: 41-63., 1971.

Glezer VD, Tsherbach TA, Gauselman VE, and Bondarko VM. Spatio-temporal organization of receptive fields of the cat striate cortex. The receptive fields as the grating filters. *Biol Cybern* 43: 35-49, 1982.

Hartveit E and Heggelund P. The effect of contrast on the visual response of lagged and nonlagged cells in the cat lateral geniculate nucleus. *Vis Neurosci* 9: 515-525., 1992.

Heeger DJ. Normalization of cell responses in cat striate cortex. *Vis Neurosci* 9: 181-197, 1992.

Horsley V and Clarke RH. The struncture and functions of the cerebellum examined by a new method. *Brain* 31: 45-124, 1908.

Hubel DH and Wiesel TN. Receptive fields, binocular interaction and functional architecture in the cat's visual cortex. *J Physiol* 160: 106-154, 1962.

Lauritzen TZ, Krukowski AE, and Miller KD. Local correlation-based circuitry can account for responses to multi-grating stimuli in a model of cat V1. *J Neurophysiol* 86: 1803-1815., 2001.

Li B, Peterson MR, Thompson JK, Duong T, and Freeman RD. Cross-orientation suppression: monoptic and dichoptic mechanisms are different. *J Neurophysiol* 94: 1645-1650, 2005.

Malpeli JG, Lee D, and Baker FH. Laminar and retinotopic organization of the macaque lateral geniculate nucleus: magnocellular and parvocellular magnification functions. *J Comp Neurol* 375: 363-377., 1996.

McLaughlin D, Shapley R, and Shelley M. Large-scale modeling of the primary visual cortex: influence of cortical architecture upon neuronal response. *J Physiol Paris* 97: 237-252., 2003.

McLaughlin D, Shapley R, Shelley M, and Wielaard DJ. A neuronal network model of macaque primary visual cortex (V1): orientation selectivity and dynamics in the input layer 4Calpha. *Proc Natl Acad Sci U S A* 97: 8087-8092., 2000.

Morrone MC, Burr DC, and Maffei L. Functional implications of cross-orientation inhibition of cortical visual cells. *Proc R Soc Lond B Biol Sci* 216: 335-354, 1982.

Morrone MC, Burr DC, and Speed HD. Cross-orientation inhibition in cat is GABA mediated. *Exp Brain Res* 67: 635-644, 1987.

Mrsic-Flogel T and Hubener M. Visual cortex: suppression by depression? *Curr Biol* 12: R547-549, 2002.

Ohzawa I, Sclar G, and Freeman RD. Contrast gain control in the cat visual cortex. *Nature* 298: 266-268, 1982.

Ohzawa I, Sclar G, and Freeman RD. Contrast gain control in the cat's visual system. *J Neurophysiol* 54: 651-667, 1985.

Palmer LA and Davis TL. Receptive-field structure in cat striate cortex. *J Neurophysiol* 46: 260-276., 1981.

Priebe NJ and Ferster D. Mechanisms underlying cross-orientation suppression in cat visual cortex. *Nat Neurosci* 9: 552-561., 2006.

Priebe NJ, Mechler F, Carandini M, and Ferster D. The contribution of spike threshold to the dichotomy of cortical simple and complex cells. *Nat Neurosci* 7: 1113-1122. Epub 2004 Aug 1129., 2004.

Reid RC and Alonso JM. Specificity of monosynaptic connections from thalamus to visual cortex. *Nature* 378: 281-284., 1995.

Sanchez-Vives MV, McCormick DA, and Nowak LG. Is synaptic depression prevalent in vivo and does it contribute to contrast adaptation? *Neuroscience conference 1998*, Los Angeles, 1998.

Sanchez-Vives MV, Nowak LG, and McCormick DA. Membrane mechanisms underlying contrast adaptation in cat area 17 in vivo. *J Neurosci* 20: 4267-4285., 2000.

Saul AB and Humphrey AL. Spatial and temporal response properties of lagged and nonlagged cells in cat lateral geniculate nucleus. *J Neurophysiol* 64: 206-224, 1990.

Sclar G and Freeman RD. Orientation selectivity in the cat's striate cortex is invariant with stimulus contrast. *Exp Brain Res* 46: 457-461, 1982.

Sclar G, Maunsell JH, and Lennie P. Coding of image contrast in central visual pathways of the macaque monkey. *Vision Res* 30: 1-10, 1990.

Sengpiel F, Baddeley RJ, Freeman TC, Harrad R, and Blakemore C. Different mechanisms underlie three inhibitory phenomena in cat area 17. *Vision Res* 38: 2067-2080, 1998.

Sengpiel F and Vorobyov V. Intracortical origins of interocular suppression in the visual cortex. *J Neurosci* 25: 6394-6400., 2005.

Shapley R, Kaplan E, and Soodak R. Spatial summation and contrast sensitivity of X and Y cells in the lateral geniculate nucleus of the macaque. *Nature* 292: 543-545., 1981.

Shapley RM and Victor JD. The effect of contrast on the transfer properties of cat retinal ganglion cells. *J Physiol* 285: 275-298., 1978.

Shapley RM and Victor JD. Nonlinear spatial summation and the contrast gain control of cat retinal ganglion cells. *J Physiol* 290: 141-161., 1979.

Shelley M and McLaughlin D. Coarse-grained reduction and analysis of a network model of cortical response: I. Drifting grating stimuli. *J Comput Neurosci* 12: 97-122., 2002.

Shelley M, McLaughlin D, Shapley R, and Wielaard J. States of high conductance in a large-scale model of the visual cortex. *J Comput Neurosci* 13: 93-109., 2002.

Shou T, Li X, Zhou Y, and Hu B. Adaptation of visually evoked responses of relay cells in the dorsal lateral geniculate nucleus of the cat following prolonged exposure to drifting gratings. *Vis Neurosci* 13: 605-613., 1996.

Smith MA, Bair W, Cavanaugh JR, and Movshon JA. Latency of inhibition from inside and outside the classical receptive field in macaque V1 neurons. *Journal of Vision* 1: 35a, 2001.

Smith MA, Bair W, and Movshon JA. Dynamics of suppression in macaque primary visual cortex. *J Neurosci* 26: 4826-4834., 2006.

Somers DC, Nelson SB, and Sur M. An emergent model of orientation selectivity in cat visual cortical simple cells. *J Neurosci* 15: 5448-5465., 1995.

Tanaka K. Organization of geniculate inputs to visual cortical cells in the cat. *Vision Res* 25: 357-364, 1985.

Tolhurst DJ and Dean AF. The effects of contrast on the linearity of spatial summation of simple cells in the cat's striate cortex. *Exp Brain Res* 79: 582-588, 1990.

Tolhurst DJ and Dean AF. Spatial summation by simple cells in the striate cortex of the cat. *Exp Brain Res* 66: 607-620, 1987.

Troyer TW, Krukowski AE, Priebe NJ, and Miller KD. Contrast-invariant orientation tuning in cat visual cortex: thalamocortical input tuning and correlation-based intracortical connectivity. *J Neurosci* 18: 5908-5927., 1998.

Varela JA, Sen K, Gibson J, Fost J, Abbott LF, and Nelson SB. A quantitative description of short-term plasticity at excitatory synapses in layer 2/3 of rat primary visual cortex. *J Neurosci* 17: 7926-7940., 1997.

Varela JA, Song S, Turrigiano GG, and Nelson SB. Differential depression at excitatory and inhibitory synapses in visual cortex. *J Neurosci* 19: 4293-4304., 1999.

Vidyasagar TR, Pei X, and Volgushev M. Multiple mechanisms underlying the orientation selectivity of visual cortical neurones. *Trends Neurosci* 19: 272-277, 1996.

Walker GA, Ohzawa I, and Freeman RD. Binocular cross-orientation suppression in the cat's striate cortex. *J Neurophysiol* 79: 227-239., 1998.

Wielaard DJ, Shelley M, McLaughlin D, and Shapley R. How simple cells are made in a nonlinear network model of the visual cortex. *J Neurosci* 21: 5203-5211., 2001.

Figure legends

Figure 1. A schematic diagram of our experimental protocol. A:The test -only condition in which an optimally oriented grating is presented for 2 seconds following a 10 second exposure to a blank screen. B: A test stimulus with a superimposed orthogonal mask (i.e., plaid). C: Following the blank screen exposure, a mask is presented for 0.5s. Then a test stimulus is presented immediately (0s delay) or after delay periods (0.5, 1, 2, and 4s). All conditions are randomly interleaved with a 10s inter-stimulus interval. The number shown below each icon indicates the duration of each stimulus presentation.

Figure 2. Recovery from COS. A: Recovery time course of COS for a cortical cell. Unfilled circles represent the mean response amplitude during the first 0.5 seconds of the response to a test stimulus following a mask. Responses are plotted as a function of the delay imposed between mask and test stimuli. Unfilled up and down triangles represent predicted responses from synaptic depression with recovery time constants of 200 and 600ms, respectively. Top and bottom horizontal dashed lines represent response levels to the test-only and to the plaid, respectively. Dotted lines and error bars show ± 1 SE. B: Normalized population average for the recovery time course of COS. Symbols are the same as in A. C: A histogram of recovery values for the 0s delay condition. Filled and unfilled circles represent simple and complex cells (n=13 and n=23, respectively). Up and down triangles represent predictions from a model of synaptic depression with 200ms and 600ms recovery time constants, respectively. Arrows represent medians of the distributions. D: The neural response time course of an example complex cell to a test-only stimulus (unfilled circles), a test stimulus following a 0.5-second mask (filled

circles), and a plaidstimul us (unfilled squares). In each case, the onset of the test stimulus begins at time zero. Each data point represents the mean spike rate for 10 repetitions of each stimulus condition. Bin sizes are 75ms. E: The mean response time course of all complex cells (n=23). Symbols are identical to those in D.

Figure 3: Contrast saturation of cells in the LGN. A: Responses of a single LGN neuron (solid line, unfilled circles, left ordinate) and corresponding contrast saturation index values (CSI) as a function of stimulus contrast (dashed line, filled circles, right ordinate). CSI increases monotonically with stimulus contrast for values above 7%. B: Distribution of CSI values for the 50% and 100% contrast response pairs are shown for a population of LGN neurons (n=74). The mean is 0.33 (arrow). C: A distribution is presented of the average CSI values for four contrast pairs, i.e., 7 and 14%, 14 and 26%, 26 and 50%, and 50 and 100%.

Figure 4: A model is depicted of contrast saturation in the LGN as a basis for COS in visual cortex. A: Standard push-pull feed-forward arrangement of LGN input to a simple cell. The simple cell receives convergent input from eight LGN cells. Four of these provide excitatory input ("push"), and the remaining four, inhibitory input ("pull") to the cortical cell via the four inhibitory interneurons illustrated. Excitatory and inhibitory inputs consist of two ON-center and two OFF-center LGN cells marked by + and – signs, respectively. The ON and OFF center cells are positioned over corresponding subfields of the cortical RFs. Excitation of an ON-center cell is balanced by an overlapping inhibition from an OFF-center cell. Orientation selectivity is generated through the elongated ON

and OFF sub-regions (dashed lines) in the RF of the simple cell. B: A schematic diagram showing how contrast saturation in the LGN can lead to COS in the model simple cell. The pattern of excitation is complemented by subtractive inhibition in a "push-pull" manner. Grating and plaid stimuli are shown in the left column. The center and right-hand columns denote relative responses from corresponding LGN cells that provide excitation and inhibition to the cortical cell. LGN response is positive (+1) if the RF of the LGN cell is in phase with the stimulus, and 0 if it is 90 or 180 degrees out of phase with the stimulus. The column of numbers on the far right denotes responses from the cortical cell calculated from the sum of the excitatory input (labeled Excitation) minus the sum of the inhibitory input (labeled Inhibition). If responses of LGN cells increase linearly with stimulus contrast, the overall response of the simple cell to a plaid is 4 (third row), which is identical to its response to the vertical grating alone. However, if LGN responses exhibit contrast saturation, the overall response of the simple cell to the plaid will be lower than 4 (bottom row). C: Comparison of the magnitude of COS predicted by the model to that measured in our study. The model simple cell gives a maximum response to the test and no response to the mask (first two bars). Compared to the response to the test stimulus, the predicted response to a plaid (third bar) of the model simple cell is clearly reduced. The fourth bar represents the mean response reduction (49%) during presentation of a plaid stimulus for our population of cortical cells (n=36).

Figure 5. COS as a function of contrast. A: Normalized response at 12.5 (dotted), 25 (dashed), and 50% (solid) test contrasts as a function of mask contrast. For all test contrasts, the level of suppression increases with mask contrast. Mask contrasts less than

10% elicit negligible suppression. B: A comparison of the mean CSI (black bars) of LGN cells, with the predicted (white bars) and measured (gray bars) levels of COS for both the mask and test at 12.5, 25, or 50% contrast.

Figure 6. Temporal frequency tuning of contrast saturation in the LGN. A: Contrast tuning curves at different temporal frequencies. Each contrast response function is independently fit with a hyperbolic function (Albrecht and Hamilton 1982). B: The contrast saturation index (filled circles) is shown as a function of temporal frequency for an example LGN cell. These data are fit with a Gaussian function (dashed line) in order to quantify the peak (TF_{peak}) and cutoff (TF_{cutoff}) temporal frequencies. The TF_{peak} and TF_{cutoff} values (arrows) for this example cell are 8.6 and 14.5Hz, respectively. The goodness of fit (R^2) for this example is 0.93. C, D: The distributions of TF_{peak} and TF_{cutoff} values for a population of 15 LGN cells. Numbers in each panel indicate the mean and standard deviation of each distribution.

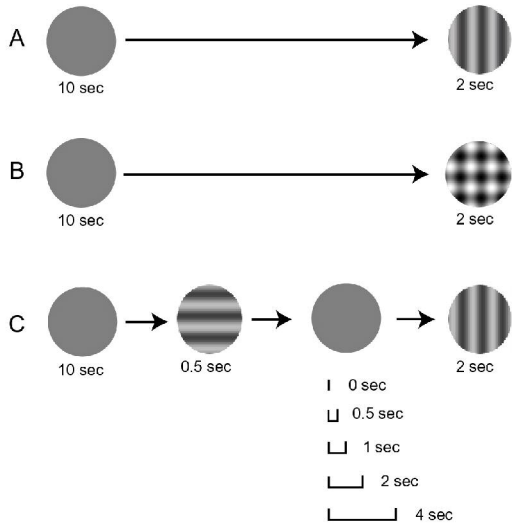
A
10 sec
2 sec
B
10 sec
2 sec
C
10 sec
0.5 sec
2 sec
0 sec
0.5 sec
1 sec
2 sec
4 sec

Fig. 1

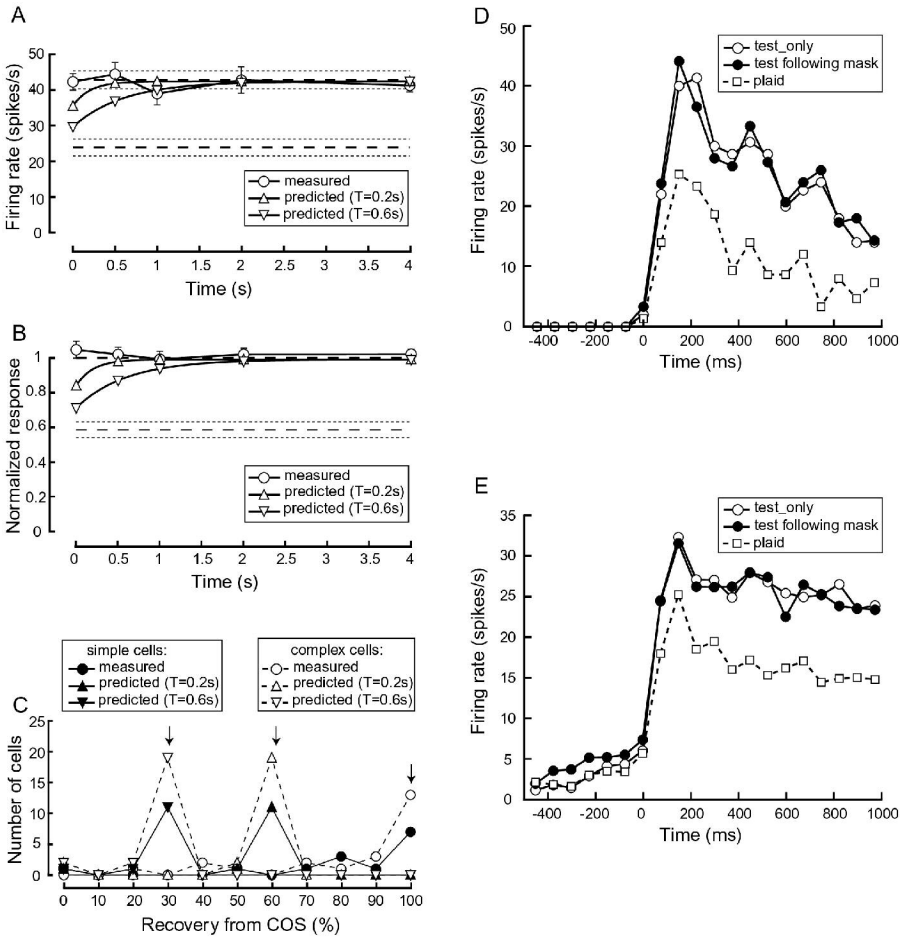
A
Firing rate (spikes/s)
Time (s)
measured
predicted (T=0.2s)
predicted (T=0.6s)
B
Normalized response
Time (s)
measured
predicted (T=0.2s)
predicted (T=0.6s)
C
Number of cells
Recovery from COS (%)
simple cells:
measured
predicted (T=0.2s)
predicted (T=0.6s)
complex cells:
measured
predicted (T=0.2s)
predicted (T=0.6s)
D
Firing rate (spikes/s)
Time (ms)
test_only
test following mask
plaid
E
Firing rate (spikes/s)
Time (ms)
test_only
test following mask
plaid

Fig. 2

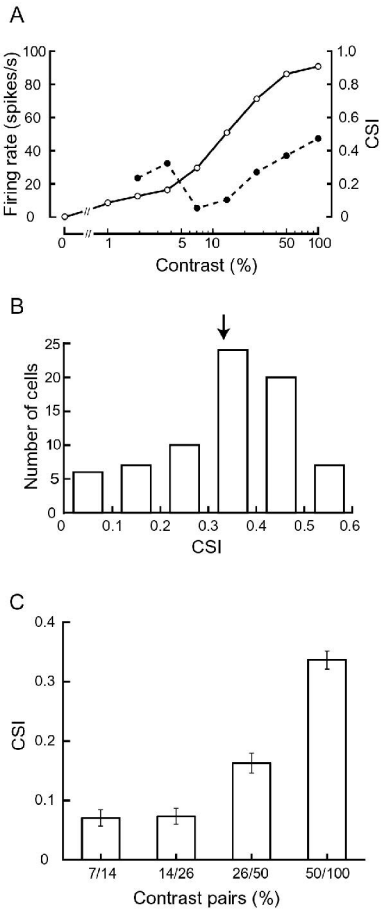
A
Firing rate (spikes/s)
CSI
Contrast (%)
B
Number of cells
CSI
C
CSI
7/14
14/26
26/50
50/100
Contrast pairs (%)

Fig. 3

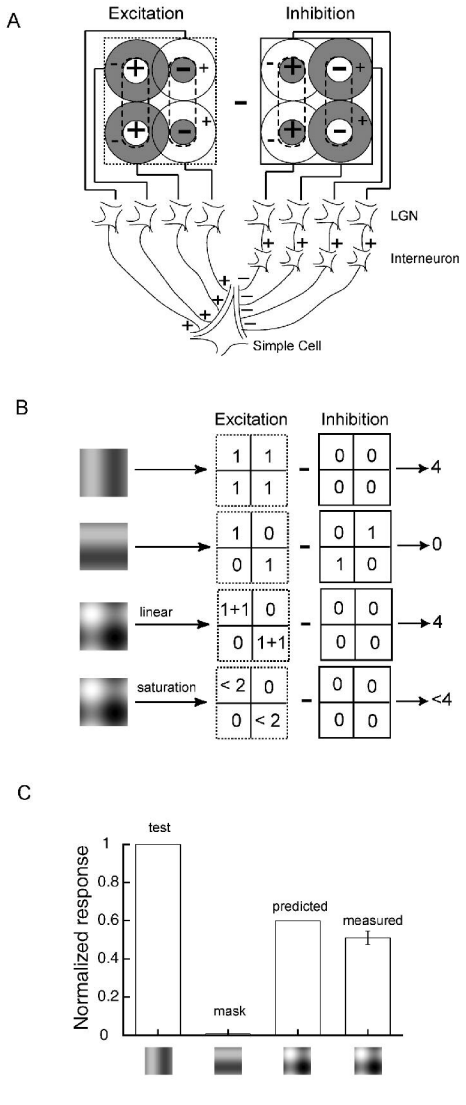
A
Excitation
Inhibition
LGN
Interneuron
Simple Cell
B
Excitation
Inhibition
1 1
1 1
0 0
0 0
4
1 0
0 1
0 1
1 0
0
linear
1+1 0
0 1+1
0 0
0 0
4
saturation
< 2 0
0 < 2
0 0
0 0
<4
C
Normalized response
1
0.8
0.6
0.4
0.2
0
test
mask
predicted
measured

Fig. 4

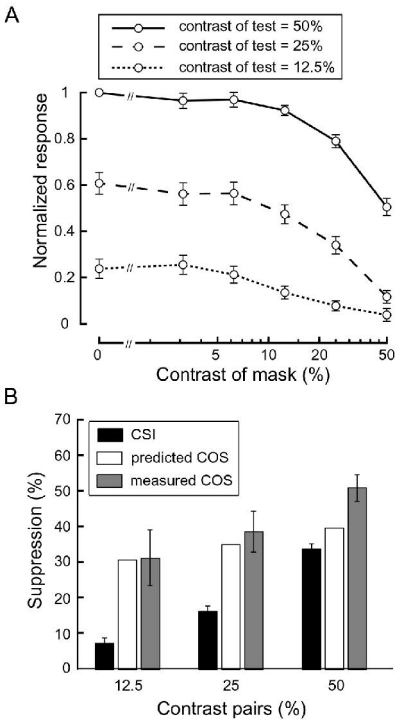
A
contrast of test = 50%
contrast of test = 25%
contrast of test = 12.5%
Normalized response
1
0.8
0.6
0.4
0.2
0
0
5
10
20
50
Contrast of mask (%)
B
CSI
predicted COS
measured COS
Suppression (%)
70
60
50
40
30
20
10
0
12.5
25
50
Contrast pairs (%)

Fig. 5

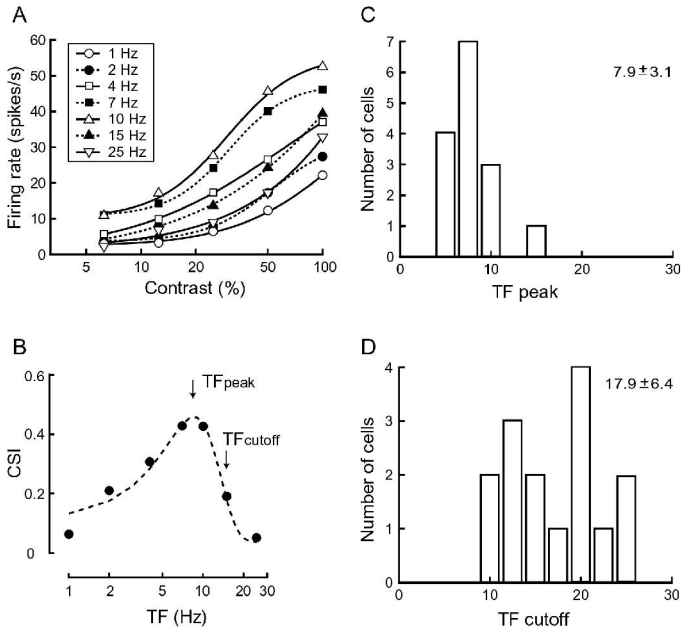
A
Firing rate (spikes/s)
Contrast (%)
1 Hz
2 Hz
4 Hz
7 Hz
10 Hz
15 Hz
25 Hz
C
Number of cells
TF peak
7.9±3.1
B
CSI
TFpeak
TFcutoff
TF (Hz)
D
Number of cells
TF cutoff
17.9±6.4

Fig. 6